Lawrence Berkeley National Laboratory

Title
Low-temperature formation of polycyclic aromatic hydrocarbons in Titan's atmosphere

Permalink
https://escholarship.org/uc/item/1pj0q014

Journal
Nature Astronomy, 2(12)

ISSN
2397-3366

Authors
Zhao, Long
Kaiser, Ralf I
Xu, Bo
et al.

Publication Date
2018-12-01

DOI
10.1038/s41550-018-0585-y

Peer reviewed

Low-Temperature Formation of Polycyclic Aromatic Hydrocarbons in Titan's Atmosphere

Long Zhao, Ralf I. Kaiser*,[1]

Department of Chemistry, University of Hawaii at Manoa, Honolulu, Hawaii, 96822

Bo Xu, Utuq Ablikim, Musahid Ahmed*,[2]

Chemical Sciences Division, Lawrence Berkeley National Laboratory, Berkeley, California 94720,

Mikhail M. Evseev, Eugene K. Bashkirov, Valeriy N. Azyazov

Samara University, Samara, 443086, Russia

Alexander M. Mebel*,[3]

Department of Chemistry and Biochemistry, Florida International University, Miami, Florida 33199 and Samara University, Samara, 443086, Russia

---

[1] To whom correspondence should be addressed. E-mail: ralfk@hawaii.edu
[2] To whom correspondence should be addressed. E-mail: mahmed@lbl.gov
[3] To whom correspondence should be addressed. E-mail: mebela@fiu.edu

Abstract

The detection of benzene in Titan's atmosphere led to the emergence of polycyclic aromatic hydrocarbons as potential nucleation agents triggering the growth of Titan's orange-brownish haze layers. However, the fundamental mechanisms leading to the formation of PAHs in Titan's low-temperature atmosphere have remained elusive. We provide persuasive evidence through laboratory experiments and computations that prototype PAHs like anthracene and phenanthrene ($C_{14}H_{10}$) are synthesized via barrier-less reactions involving naphthyl radicals ($C_{10}H_7^{\bullet}$) with vinylacetylene ($CH_2=CH-C\equiv CH$) in low-temperature environments. These elementary reactions are rapid, have no entrance barriers, and synthesize anthracene and phenanthrene via van-der-Waals complexes and submerged barriers. This facile route to anthracene and phenanthrene – potential building blocks to complex PAHs and aerosols in Titan - signifies a critical shift in the perception that PAHs can be only formed at high-temperature conditions providing a detailed understanding of the chemistry of Titan's atmosphere through untangling elementary reactions on the most fundamental level.

The Cassini-Huygens mission to Saturn's moon Titan – the only Solar System body besides Earth sustaining a dense, nitrogen-rich atmosphere and solid surface – has transformed our knowledge of the origin and evolution of the Solar System[1,2]. Titan's most prominent optically visible features are the aerosol-based haze layers, which define its orange-brownish color. These layers, composed of aerosol particles, are essential to Titan's climate, radiation balance and atmospheric chemistry. Polycyclic aromatic hydrocarbons (PAHs) have been the center of attention as prospective candidates that initiate formation and growth of complex organics in Titan's orange-brownish haze layers[3]. The existence of PAHs in Titan's atmosphere has been inferred from Cassini's Visual and Infrared Mapping Spectrometer (VIMS) attributing the 3.28 µm (3049 cm^{-1}) absorption to stratospheric PAHs[4] following an earlier PAH assignment in the upper atmosphere up to 1,300 km.[5] Likewise, Cassini's Plasma Spectrometer (CAPS) detected heavy positively (< 350 Da) and negatively (< 8,000 Da) charged particles, which have been proposed to carry PAHs,[6] possibly formed via reactions involving benzene (C_6H_6) and phenyl radical ($C_6H_5^•$) in atmospheric regions between 350 and 1,200 km[7]. The most fundamental building block of all PAHs – the benzene molecule – was observed in Titan's atmosphere at levels of up to 10 ppm.[8-13] These levels might signify benzene and possibly heavier, but hitherto undetected aromatics like naphthalene ($C_{10}H_8$) and anthracene/phenanthrene ($C_{14}H_{10}$) as key building blocks participating in the growth processes to complex PAHs. However, there is a lack of understanding as to the molecular mechanisms which initiate and drive formation of PAHs in Titan's low temperature atmosphere (70 K to 180 K).[14]

Popular routes to PAH formation on Titan have been derived from high temperature combustion models and suggest sequential reactions of aromatic (phenyl; $C_6H_5^•$)[14-17] and resonantly stabilized radicals (propargyl; $C_3H_3^•$)[18]. Together with acetylene (C_2H_2), these reactions constitute the backbone for a recurring sequence of hydrogen abstraction – acetylene addition (HACA) mechanism operating at elevated temperatures of up to 1,000 K leading to facile synthesis of naphthalene ($C_{10}H_8$)[19-22]. However, unsurmountable entrance barriers to addition up to 20 kJ mol^{-1} cannot be passed under Titan's low temperature conditions (70–200 K)[23] leading to a challenge to the traditional HACA con-cept[24,25]. Parker et al. revealed that naphthalene ($C_{10}H_8$) can be synthesized via a *barrier-less* reactions at temperatures as low as 10 K involving a bimolecular reaction between the phenyl radical ($C_6H_5^•$) and vinylacetylene (C_4H_4)[17] through the hydrogen abstraction – vinylacetylene addition (HAVA) pathway[17,26-29]. Since the solar ultraviolet radiation penetrates deep into Titan's atmosphere[30], benzene (C_6H_6) photodissociates to the phenyl radical ($C_6H_5^•$) plus atomic hydrogen ($H^•$)[31]. Along with phenyl, the naphthyl radical ($C_{10}H_7^•$) generated via photodissociation of naphthalene ($C_{10}H_8$),

3

may initiate a barrier-less, vinylacetylene-mediated low temperature chemistry involving these aryl-type radicals and leading to naphthalene ($C_{10}H_8$) and anthracene/phenanthrene ($C_{14}H_{10}$) (Figure 1). However, the validity of these mass growth processes beyond naphthalene has remained conjectural, since not a single laboratory experiment has been performed to corroborate to what extent complex PAHs like anthracene ($C_{14}H_{10}$) and phenanthrene ($C_{14}H_{10}$) can be synthesized in these barrier-less processes. Therefore, the proposed omnipresence of PAHs in Titan's haze layers[5], but the lack of validated laboratory experiments demonstrating the synthesis of PAHs under Titan's low temperature conditions and how they chemically link to Titan's haze layers represent a fundamental enigma to the planetary science and reaction dynamics communities. Sophisticated laboratory experiments simulating the formation of aerosols under the conditions of Titan's atmosphere using vacuum ultraviolet light irradiation consistently detected vinylacetylene.[32,33] Also, crossed molecular beam experiments demonstrated that vinylacetylene is formed in the photolysis of acetylene[34,35] and in the reaction of the ethynyl radical (C_2H) with ethylene (C_2H_4), with these species being among the most abundant hydrocarbons in the atmosphere of Titan.[36] Finally, photochemical models of Titan's atmosphere reveal that vinylacetylene prevails at mixing ratios exceeding 10^{-6}-10^{-5}.[37-39]

Here, we report the results of the bimolecular gas phase reactions of the 1- and 2-naphthyl radical [$C_{10}H_7^{\bullet}$; 127 amu; X^2A_1] with vinylacetylene [$CH_2=CH-C\equiv CH$; 52 amu; X^1A'] (Figure 1). By merging the experiments with electronic structure and statistical calculations, we present evidence of a *barrier-less* formation of two prototype tricyclic PAHs - anthracene [$C_{14}H_{10}$; 178 amu; X^1A_1] and phenanthrene [$C_{14}H_{10}$; 178 amu; X^1A_1] - involving van-der-Waals complexes and submerged barriers to reaction in the entrance channels. These barrier-less pathways defy conventional wisdom that PAH formation such as to anthracene and phenanthrene solely transpires in high-temperature environments such as in combustion flames. This facile route via bimolecular mass growth processes in low temperature environments such as in Titan's atmosphere involving vinylacetylene defines an essential shift in currently 'well-established' perceptions leading to PAHs, which have so far relied exclusive on a high-temperature, acetylene-based chemistry (HACA).[19-22,24,40] The combination of laboratory experiments with electronic structure calculations lead to an unraveling of the chemistry of elementary reactions leading to PAHs at the microscopic level, via a hitherto overlooked vinylacetylene-mediated mass growth processes to PAHs at ultralow temperatures, thus providing a detailed chemical understanding of a macroscopic environment – Saturn's moon Titan.

Results - Experimental Studies

4

A chemical reactor was utilized to explore the synthesis of anthracene ($C_{14}H_{10}$) and phenanthrene ($C_{14}H_{10}$) via the elementary reactions of the 1- and 2-naphthyl radicals ($C_{10}H_7^\bullet$) with vinylacetylene (Figure 1). The products were entrained in a molecular beam, ionized via fragment free, soft photoionization utilizing synchrotron vacuum ultraviolet light, and detected isomer-specifically with a reflectron time-of-flight mass spectrometer (PI-ReTOF-MS) (Materials & Methods). Representative mass spectra recorded at a photoionization energy of 9.50 eV for the reaction of the 1- and 2-naphthyl radicals with vinylacetylene are displayed in Figure 2. Reference spectra were also collected by replacing vinylacetylene with non-reactive helium carrier gas (Figure 2). These data provide convincing evidence on the synthesis of molecules with the molecular formula $C_{14}H_{10}$ (178 amu) in the 1- and 2-naphthyl – vinylacetylene systems, which are absent in the control experiments. Accounting for the molecular weights of the reactants ($C_{10}H_7^\bullet$, 127 amu; C_4H_4, 52 amu) and the products ($C_{14}H_{10}$, 178 amu; H, 1 amu), the molecules with the formula $C_{14}H_{10}$ must be the reaction products of the bimolecular reaction of the 1- and 2-naphthyl radicals with vinylacetylene (Figure 1). Signal associated with ion counts at mass-to-charge (m/z) of 152 can be linked with the reaction of the 1- and 2-naphthyl radicals (127 amu) with acetylene (C_2H_2; 26 amu) and the inherent formation of acenaphthylene ($C_{12}H_8$) and ethynylnaphthalene isomers ($C_{12}H_8$) (Supplementary Figures 1-3). Finally, ion counts at m/z = 209 ($C_9^{13}CH_7{}^{81}Br^+$), 208 ($C_{10}H_7{}^{81}Br^+$), 207 ($C_9^{13}CH_7{}^{79}Br^+$), 206 ($C_{10}H_7{}^{79}Br^+$), 129 ($C_9^{13}CH_8^+$), 128 ($C_{10}H_8^+$), 127 ($C_{10}H_7^+/C_9^{13}CH_6^+$), and 126 ($C_{10}H_6^+$) are also observable in the 1- and 2-naphthyl – helium systems. Hence, these masses do not originate from reactions between 1- and 2-naphthyl radicals and vinylacetylene. Signal between m/z = 209 to 206 can be associated with the non-pyrolyzed 1- and 2-bromonaphthalene precursor; signal at m/z = 128 and 129 is attributed to naphthalene and ^{13}C-naphthalene formed via atomic hydrogen addition to the 1- and 2-naphthyl radicals. The ion counts at m/z = 127 are linked to 1- and 2-naphthyl radicals ($C_{10}H_7^+$), while ions at m/z = 126 are associated with naphthyne isomers ($C_{10}H_6^+$) (Supplementary Figures 2 and 3). To summarize, the analysis of the mass spectra reveals that the reaction of the 1- and 2-naphthyl radicals ($C_{10}H_7^\bullet$) with vinylacetylene (C_4H_4) synthesizes hydrocarbon molecule(s) with the molecular formula $C_{14}H_{10}$.

With the detection of hydrocarbon molecule(s) of the molecular formula $C_{14}H_{10}$ via the reaction of the 1- and 2-naphthyl radicals with vinylacetylene, it is our objective to assign the structural isomer(s) formed in these elementary reactions (Figure 1). This necessitates a detailed analysis of the corresponding photoionization efficiency (PIE) curves, which report the intensity of the ions at m/z = 178 ($C_{14}H_{10}^+$) as a function of the photon energy from 7.20 eV to 9.50 eV (Figure 3). These data are

5

fit with newly recorded reference PIE curves for distinct $C_{14}H_{10}$ isomers (anthracene and phenanthrene) (Supplementary Figure 4). The experimentally derived PIE curves at $m/z = 178$ (black) can be reproduced effectively by a linear combination of two reference PIE curves of anthracene ($C_{14}H_{10}$; blue) and phenanthrene ($C_{14}H_{10}$; green) with the overall fit exhibited in red (Figures 3a and 3c). The experimental PIE curves for $m/z = 178$ illustrate both onsets of the ion signal at 7.40 ± 0.05 eV. This onset correlates nicely with the adiabatic ionization energy of anthracene of 7.44 eV.[41] The adiabatic ionization energy of phenanthrene was determined to be 7.90 eV.[42] Moreover, both PIE curves of $m/z = 179$ could be reproduced with a linear combination of anthracene and phenanthrene (Figs. 3b and 3d). Consequently, signal at $m/z = 179$ can be associated with ^{13}C substituted anthracene and phenanthrene ($C_{13}{}^{13}CH_{10}$). The PIE curves of distinct $C_{14}H_{10}$ isomers are *linked* to individual molecules underlining that the co-existence of other isomers in the molecular beam would change the shape of the PIE considerably and hence can be excluded. Therefore, we conclude that within our error limits, anthracene and phenanthrene denote the only contributions to signal at $m/z = 178$ and 179. Accounting for the ionization cross sections of phenanthrene and anthracene, branching ratios of $89:11(\pm10\%)$ and $80:20(\pm10\%)$ are derived for the 1-naphthyl and 2-naphthyl systems, respectively, i.e. a dominant formation of the thermodynamically more stable phenanthrene isomer.

Results - Electronic Structure Calculations & Reaction Mechanism

The present study reveals for the very first time that two prototype PAHs composed of three benzene rings – phenanthrene and anthracene – can be synthesized via the elementary reactions of the 1- and 2-naphthyl radicals with vinylacetylene in the gas phase. We are merging now these findings with the computational results to untangle the underlying reaction mechanism(s) (Figure 4) (Materials & Methods; Supplementary Figure 5). For each the 1-naphthyl-vinylacetylene and the 2-naphthyl-vinylacetylene systems, our electronic structure calculations revealed two entrance channels to addition, among them one de facto barrier-less pathway. All reactions are initiated by addition of the radical center of the naphthyl radical to the terminal C1 or C4 carbon atom of the vinylacetylene reactant carrying the acetylenic (HCC-) and vinyl moieties (H2CCH-), respectively, via van-der-Waals complexes [1]–[4] weakly bound by 9 to 12 kJ mol⁻¹. For each complex, a closer approach of the radical center leads to the formation of a covalent carbon-carbon bond and, hence, intermediates [5]–[8] via barriers of 7 to 13 kJ mol⁻¹. The addition of the 1- and 2-naphthyl radicals to the C4 carbon atom leads to resonantly stabilized free radical (RSFR) intermediates [5] and [7] and the transition states to addition lie lower in energy that the separated reactants. Therefore, a barrier to addition exists, but since this barrier is located below the energy of the reactants, it is a *submerged barrier*. For the

overall reaction of naphthyl plus vinylacetylene to the $C_{14}H_{11}$ intermediates [5] and [7], the reaction is de facto barrier less. This is in strong contrast to the addition of the 1- and 2-naphthyl radicals to the C1 carbon atom forming intermediates [6] and [8]. The transition states to addition reside above the energy of the separated reactants and hence a barrier to addition does exist at the C1 atom of vinylacetylene.

Within the 1-naphthyl-vinylacetylene system, intermediate [5] undergoes a [1,4] hydrogen shift from the *ortho* carbon of the ring to the β carbon of the side chain forming [9], followed by cyclization to gain the phenanthrene carbon backbone in [10], hydrogen shift to the carbene center yielding [11], and ultimately atomic hydrogen loss from the CH_2 moiety followed by aromatization and formation of phenanthrene (**p1**) via a tight exit transition state in an overall exoergic reaction (-277 kJ mol^{-1}). All pertinent transition states leading to the formation of phenanthrene in the reaction sequence [1]→[5]→[9]→[10]→[11]→**p1** + H are below the energy of the separated reactants and hence accessible even at ultralow temperatures. Radical intermediate [6], which can only be accessed at elevated temperatures due to the inherent addition barrier, can eventually react to anthracene (**p2**) in an overall exoergic reaction (-254 kJ mol^{-1}) via seven isomerization steps from [6] to [12]→[13]→[8]→[14]→[15]→[16]→[17] via [1,4] hydrogen shift from the ring to the side chain, migration of the former vinylacetylene moiety from the C1 to the C2 carbon atom of naphthalene, two more [1,4] H shifts first from the side chain back to the radical site of the ring and then from the other ring to the side chain, cis-trans isomerization via a tricyclic intermediate, followed by the four-member ring opening and six-member ring closure to form the anthracene carbon backbone in [17] and completed by an H loss from the CH_2 moiety producing anthracene (**p2**) through a tight exit transition state in an overall exoergic reaction (-254 kJ mol^{-1}).

The 2-naphthyl-vinylacetylene system also connects both to the phenanthrene (**p1**) and anthracene (**p2**) isomers. Initiated by intermediates [7] and [8], the reaction sequence [7]→[18]→[19]→[17] leads via [1,4] hydrogen shift, cyclization to the anthracene carbon skeleton, hydrogen migration from the CH_2 moiety to the carbene center, and hydrogen loss to anthracene (**p2**). On the other hand, the rearrangement of [7] via [20]→[21]→[22] through [1,4] hydrogen migration, cyclization, hydrogen atom migration to the carbene center, followed by atomic hydrogen elimination forms phenanthrene (**p1**). The two [1,4] hydrogen shifts in the phenanthrene and anthracene pathways take place from C1 and C3 carbons of the former 2-naphthyl moiety. Therefore, the 2-naphthyl – vinylacetylene system may essentially undergo ring closure to the C1 or the C3 carbon atoms of the naphthyl moiety leading
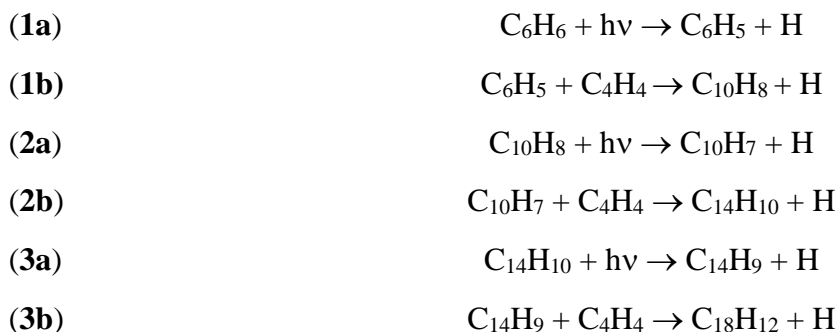
7

to phenanthrene (**p1**) and anthracene (**p2**), respectively. However, although in the 1-naphthyl – vinylacetylene system, the radical center resides initially at the C1 atom of the naphthyl radical and reaction with vinylacetylene should essentially lead only to phenanthrene (**p1**), our calculations identify – as verified experimentally - a potential shift of the radical center from the C1 to the C2 carbon atom, which in turn also allows the formation of anthracene (**p2**). It should be noted that these ring-closure mechanisms also operate for substituted naphthalenes as proposed by Zwier et al. with reactions initiated by, e.g., addition of propargyl radicals to benzyl radicals followed by photoexcitation and reaction of the primary reaction products under Titan-like conditions.[43]

To summarize, our calculations revealed de facto two barrier-less pathways to form anthracene (**p1**) and phenanthrene (**p2**) in the reactions of vinylacetylene with 1- and 2-naphthyl radicals involving van-der-Waals complexes and submerged barriers to addition. Due to the essential barrier-less nature of these reactions, both pathways involving van-der-Waals complexes [1] and [3] can lead to the synthesis of anthracene (**p1**) and phenanthrene (**p2**) in low temperature environments such as in Titan's atmosphere, whereas two alternative routes initiated by van-der-Waals complexes [2] and [4] require elevated temperatures as prevalent in combustion flames. At low temperature (collision energy) and within the limit of zero pressure, the reactions of the 1- and 2-naphthyl radical with vinylacetylene are initiated via barrier-less additions of the radical center to the terminal CH_2 moiety of the vinylacetylene reactant leading to resonantly stabilized free radical intermediates [5] and [7]. At the vinyl group, these additions commence with the formation of long range van-der-Waals complexes [1] and [3], respectively, which isomerize via submerged barriers to [5] and [7]. These intermediates eventually isomerize via successive hydrogen migrations followed by ring closure to ultimately form both anthracene (**p1**) and phenanthrene (**p2**) via tight exit transition states through hydrogen atom elimination. These tight exit transition states can be rationalized easily since the reversed reactions, i.e. the addition of a hydrogen atom to a closed shell 14π aromatic electron system is associated with an entrance barrier similar to the reaction of atomic hydrogen with benzene (37 kJ mol^{-1})[44] and naphthalene (24 kJ mol^{-1})[17]. Due to the essential barrier-less nature of these bimolecular reactions, both pathways involving van-der-Waals complexes [1] and [3] lead to the synthesis of anthracene (**p1**) and phenanthrene (**p2**) in low temperature environments, whereas two alternative routes initiated by van-der-Waals complexes [2] and [4] require elevated temperatures as prevalent in combustion flames.

Discussion – Titan's Atmosphere

Having demonstrated the facile synthesis of anthracene (**p1**) and phenanthrene (**p2**) via molecular mass growth processes involving ring expansion through de facto *barrier-less* reactions of aromatic radicals (naphthyl) with vinylacetylene, we transfer our findings from the laboratory and computer to the atmosphere of Saturn's moon Titan. The absence of any entrance barrier in a bimolecular reaction represents a crucial prerequisite for a chemical reaction to be feasible under the extreme low temperature conditions in Titan's atmosphere (70–180 K). These low temperatures typically block reactions that have a significant entrance barrier such as the pathways via intermediates [2] and [4] shown in the present study. Consequently, chemical reactions relevant to Titan's atmosphere must be exoergic, proceed without an entrance barrier, and must only involve transition states that are lower than the energy of the separated reactants. All these benchmarks are fulfilled in the bimolecular reactions of the 1- and 2-naphthyl radicals with vinylacetylene leading to anthracene (**p1**) and phenanthrene (**p2**) (Figure 4, blue pathways). We would like to emphasize that the temperature in our experiments is higher than in Titan's atmosphere. Likewise, the pressure conditions differ from 300 Torr in the entrance of our reactor to close to 100 Torr in the relevant atmospheric range in Titan; these ranges correspond to altitudes from 30 to 50 km in Titan's atmosphere.[10] Do these discrepancies have any influence on the implications of the formation of anthracene (**p1**) and phenanthrene (**p2**) on Titan? At higher temperatures, additional pathways can open up, if the barrier to hydrogen abstraction forming naphthyl ($C_{10}H_7^{\bullet}$) and, for instance, 1-vinyl-ethyn-1-yl (H_2CCCCH) can be overcome. Likewise, pathways via intermediates [2] and [4] are accessible at elevated temperatures if the barriers to addition can be passed. Nevertheless, these additional channel does not change the reaction mechanism to form anthracene and phenanthrene via intermediates [1] and [3], and we have to conclude that at the low temperature conditions of Titan and at the high temperatures prevailing in our experiments, both anthracene (**p1**) and phenanthrene (**p2**) can be formed, albeit with different rate constants and at different branching ratios (Supplementary Table 1).

Our results predict critical trends in Titan's atmosphere leading ultimately to mass growth processes of PAHs on the molecular level. *First*, starting with the phenyl radical ($C_6H_5^{\bullet}$), PAHs of the generic formulae $C_{(10+4n)}H_{(8+2n)}$ with naphthalene (n=0), anthracene/phenanthrene (n=1), and, e.g. tetracene (n=2), are predicted to be readily formed in the atmosphere of Titan via stepwise molecular mass growth sequences via reactions of phenyl ($C_6H_5^{\bullet}$), naphthyl ($C_{10}H_7^{\bullet}$), and anthracenyl ($C_{14}H_9^{\bullet}$) with vinylacetylene (C_4H_4) (reactions **1-3**). This mechanism contains two steps: the photolysis of the radical precursor (reactions **1a**, **2a**, **3a**) and a molecular mass growth through a barrier-less reaction with vinylacetylene (reactions **1b**, **2b**, **3b**) leading effectively to a PAH growth plus atomic hydrogen.

9

(**1a**)	$C_6H_6 + h\nu \rightarrow C_6H_5 + H$
(**1b**)	$C_6H_5 + C_4H_4 \rightarrow C_{10}H_8 + H$
(**2a**)	$C_{10}H_8 + h\nu \rightarrow C_{10}H_7 + H$
(**2b**)	$C_{10}H_7 + C_4H_4 \rightarrow C_{14}H_{10} + H$
(**3a**)	$C_{14}H_{10} + h\nu \rightarrow C_{14}H_9 + H$
(**3b**)	$C_{14}H_9 + C_4H_4 \rightarrow C_{18}H_{12} + H$

This growth sequence is assisted by two factors: the lack of reaction barriers discussed in this article for the reaction of naphthyl radicals with vinylacetylene and the escape of hydrogen atoms from the atmosphere of Titan as a consequence of its low gravity. Here, the production of PAHs is anticipated to be substantial throughout Titan's atmosphere considering the photolysis of low molecular mass PAH precursors such as benzene and naphthalene mainly by UV photons, where there is no or little shielding by the major constituents of Titan's atmosphere such as molecular nitrogen (N_2) and methane (CH_4). Consequently, once a PAH is formed in Titan's atmosphere via the aryl – vinylacetylene reaction, this PAH gains one six-membered ring compared to its aryl precursor. This molecular mass growth process can continue by photolysis of the newly formed PAH to its corresponding aryl reactants, which then reacts with another vinylacetylene molecule to an even more complex PAH. This molecular mass growth may continue until the PAH agglomerates into the aerosol-based hazed layer or precipitates onto Titan's surface. Lopez-Puertas et al.[5] proposed that up to 19 PAHs – including phenanthrene and anthracene as molecular building blocks - represent a 'best fit' to the VIMS emission spectra in Titan's atmosphere. This finding correlates nicely with previous studies by Sagan et al.[3] suggesting that phenanthrene and anthracene act as molecular carriers of tholins produced in Titan's atmosphere. Finally, Ali et al.[45] analyzed data of Titan's upper atmosphere obtained by the Cassini Ion and Neutral Mass Spectrometer (INMS) concluding that nitrogen substituted phenanthrene likely acts as a major contributor to Titan's haze precursors. Therefore, the 1-/2-naphthyl – vinylacetylene system represents a critical proof-of-concept study that elementary PAH growth processes may drive the low temperature chemistry of complex aromatic molecules in Titan's atmosphere, providing an explanation for the potential presence of not only naphthalene, anthracene and phenanthrene as building blocks to even more complex PAHs in Titan's atmosphere. The transition from naphthalene[17] to anthracene/phenanthrene and heavier PAHs via reactions (1) to (3) involving the barrier-less HAVA mechanism represents thus a critical, hitherto ignored reaction

sequence to build up complex PAHs via stepwise molecular mass growth processes at low temperatures in Titan's atmospheres.

Summary

To summarize, our experimental study identified anthracene and phenanthrene as key reaction products of the elementary reactions of the 1-/2-naphthyl radical with vinylacetylene. The reaction channels display no entrance barrier, are exoergic, and all transition states involved are located below the energy of the separated reactant molecules. Considering these features, the bimolecular reactions of the naphthyl radicals with vinylacetylene reveal a facile pathway to synthesize anthracene and phenanthrene in Titan's atmosphere in those regions, where density profiles of photolytically generated naphthyl radicals and vinylacetylene intersect. These findings further propose that successive reactions of anthracene and phenanthrene molecule can synthesize even more complex PAHs via the HAVA mechanism. Here, anthracenyl or phenanthrenyl radicals ($C_{14}H_9^{\bullet}$) generated via photodissociation of anthracene or phenanthrene ($C_{14}H_{10}$), respectively, could react with vinylacetylene to five possible PAHs carrying four six-membered rings such as benz[*a*]anthracene, tetracene, chrysene, benzo[*c*]phenanthrene and triphenylene. These data provide critical sinks of PAHs for the organic aerosol layers and also provide a scientific groundwork for the previously tentative spectroscopic assignments of PAHs in Titan's atmosphere via Cassini's VIMS at 3.28 µm (3049 cm^{-1})[4] thus providing crucial data to constrain the composition and density of minor neutral molecules in Titan's atmosphere and how they can be linked to the orange-brownish aerosol layers ultimately changing our paradigm that PAH can be solely formed in high temperature environments via HACA[19-22,24,40] or via barrier-less ion-molecule reactions[17,26-29,46]. Therefore, we suggest that our combined experimental and computational study provides a template for a warranted investigation of the low temperature organic chemistry of PAHs in Titan's atmosphere so that a comprehensive picture of the overall processes involved in the chemistry of Titan's atmosphere can emerge.

Methods - Experimental: The experiments were conducted at the Advanced Light Source (ALS) at the Chemical Dynamics Beamline (9.0.2.) exploiting a high-temperature chemical reactor consisting of a resistively-heated silicon carbide (SiC) tube of 20 mm length and 1 mm inner diameter[21,40,47]. This reactor is incorporated into a molecular beam apparatus operated with a Wiley-McLaren Re-TOF-MS[20-22,40,47-49]. This setup investigates discrete chemical reactions to simulate PAH growth *in situ* through the reaction of radicals. 1-/2- naphthyl radical ($C_{10}H_7^•$) was prepared at concentration of less than 0.1% *in situ* via pyrolysis of the 1-/2-bromonaphthalene precursor ($C_{10}H_7Br$, TCI-America, > 95% for 1-bromonaphthalene and > 98% 2-bromonaphthalene) seeded in vinylacetylene/helium (5% C_4H_4; 95% He; Applied Gas) carrier gas at the pressure of 300 Torr. The temperature of the SiC tube was monitored using a Type-C thermocouple and was maintained at $1,450 \pm 10$ K. At this temperature, 1-/2-bromonaphthalene dissociates to atomic bromine plus the 1-/2-naphthyl radical *in situ*, which then reacts with vinylacetylene. The reaction products synthesized in the reactor were expanded supersonically and passed through a 2-mm diameter skimmer located 10 mm downstream the pyrolytic reactor and enter into the main chamber, which houses the Re-TOF-MS. The products within the supersonic beam were then photoionized in the extraction region of the spectrometer by exploiting quasi-continuous tunable synchrotron vacuum ultraviolet (VUV) light and detected with a microchannel plate (MCP). It is important to highlight that VUV single photon ionization represents essentially a fragment-free ionization technique and hence is characterized as a *soft ionization* method[50,51] compared to electron impact ionization, which the latter leading to excessive fragmentation of the parent ion. The ions formed via photoionization are extracted and fed onto a microchannel plate detector through an ion lens. Photoionization efficiency (PIE) curves, which report ion counts as a function of photon energy from 7.20 eV to 9.50 eV with a step interval of 0.05 eV at a well-defined mass-to-charge ratio (*m/z*), were produced by integrating the signal recorded at the specific *m/z* for the species of interest and normalized to the incident photon flux. The residence time in the reactor tube under our experimental condition are up to hundreds of μs[52]. Reference (blank) experiments were also conducted by expanding neat helium carrier gas with the 1/2-bromonaphthalene precursor into the resistively-heated SiC tube. No signals at *m/z* = 178 or 179 were observed in these control experiments.

Methods - Electronic Structure and Rate Constant Calculations: The energies and molecular parameters of the local minima and transition states involved in the reaction were computed at the G3(MP2,CC)// B3LYP/6-311G(d,p) level of theory[53-55] within a chemical accuracy of 3–6 kJ mol^{-1} for the relative energies and 0.01–0.02 Å for bond lengths as well as 1–2° for bond angles[55]. The

GAUSSIAN 09[56] and MOLPRO 2010 program packages[57] were utilized for the ab initio calculations. The MESS package[58] was exploited to solve the one-dimensional master equation and to compute temperature-dependent rate constants in the zero- and high pressure limits within the Rice-Rampsberger-Kassel-Marcus Master Equation (RRKM-ME) method. The Rigid-Rotor, Harmonic-Oscillator (RRHO) model was utilized to compute densities of states and partition functions of local minima and numbers of states of transition states. RRKM-ME calculations at low temperatures in the 70 – 180 K range relevant to the atmosphere of Titan took into account radiative stabilization of various reaction intermediates through emission of infrared photons.

References:

1   Lorenz, R. & Mitton, J. *Titan Unveiled: Saturn's Mysterious Moon Explored*. Ch. 2 (Princeton University Press, 2010).

2   Brown, R., Lebreton, J. P. & Waite, J. H. *Titan from Cassini-Huygens*. Ch. 7 (Springer Science & Business Media, 2009).

3   Sagan, C. *et al.* Polycyclic aromatic hydrocarbons in the atmospheres of Titan and Jupiter. *Astrophys. J.* **414,** 399-405 (1993).

4   Delitsky, M. L. & McKay, C. P. The photochemical products of benzene in Titan's upper atmosphere. *Icarus* **207,** 477-484 (2010).

5   Lopez-Puertas, M. *et al.* Large abundances of polycyclic aromatic hydrocarbons in Titan's upper atmosphere. *Astrophys. J.* **770,** 132-139 (2013).

6   Jonker, M. T. O., Hawthorne, S. B. & Koelmans, A. A. Extremely slowly desorbing polycyclic aromatic hydrocarbons from soot and soot-like materials: Evidence by supercritical fluid extraction. *Environ. Sci. Technol.* **39,** 7889-7895 (2005).

7   Trainer, M. G., Sebree, J. A., Heidi Yoon, Y. & Tolbert, M. A. The influence of benzene as a trace reactant in Titan aerosol analogs. *Astrophys. J., Lett.* **766,** L4/1-L4/5 (2013).

8   Coustenis, A. *et al.* Titan's atmosphere from ISO mid-infrared spectroscopy. *Icarus* **161,** 383-403 (2003).

9   Capalbo, F. J. *et al.* New benzene absorption cross sections in the VUV, relevance for Titan's upper atmosphere. *Icarus* **265,** 95-109 (2016).

10   Vinatier, S. *et al.* Analysis of Cassini/CIRS limb spectra of Titan acquired during the nominal mission: I. Hydrocarbons, nitriles and CO_2 vertical mixing ratio profiles. *Icarus* **205,** 559-570 (2010).

11   Vinatier, S. *et al.* Study of Titan's fall southern stratospheric polar cloud composition with Cassini/CIRS: Detection of benzene ice. *Icarus*, Preprint at https://doi.org/10.1016/j.icarus.2017.1012.1040 (2018).

12   Coustenis, A. *et al.* The composition of Titan's stratosphere from Cassini/CIRS mid-infrared spectra. *Icarus* **189,** 35-62 (2007).

13   Cui, J. *et al.* Analysis of Titan's neutral upper atmosphere from Cassini Ion Neutral Mass Spectrometer measurements. *Icarus* **200,** 581-615 (2009).

14   Wilson, E. H. & Atreya, S. K. Chemical sources of haze formation in Titan's atmosphere. *Planet. Space Sci.* **51,** 1017-1033 (2003).

15   Landera, A. & Mebel, A. M. Mechanisms of formation of nitrogen-containing polycyclic aromatic compounds in low-temperature environments of planetary atmospheres: a theoretical study. *Faraday Discuss.* **147,** 479-494 (2010).

16   Kaiser, R. I., Asvany, O. & Lee, Y. T. Crossed beam investigation of elementary reactions relevant to the formation of polycyclic aromatic hydrocarbon (PAH)-like molecules in extraterrestrial environments. *Planet. Space Sci.* **48,** 483-492 (2000).

17   Parker, D. S. *et al.* Low temperature formation of naphthalene and its role in the synthesis of PAHs (polycyclic aromatic hydrocarbons) in the interstellar medium. *Proc. Natl. Acad. Sci. USA* **109,** 53-58 (2012).

18   Wilson, E. H., Atreya, S. K. & Coustenis, A. Mechanisms for the formation of benzene in the atmosphere of Titan. *J. Geophys. Res.: Planets* **108,** 8/1-8/10 (2003).

19   Frenklach, M. & Feigelson, E. D. Formation of polycyclic aromatic hydrocarbons in circumstellar envelopes. *Astrophys. J.* **341,** 372-384 (1989).

20   Parker, D. S., Kaiser, R. I., Troy, T. P. & Ahmed, M. Hydrogen Abstraction/Acetylene Addition revealed. *Angew. Chem. Int. Edit.* **53,** 7740-7744 (2014).

21   Parker, D. S. N. *et al.* Unexpected chemistry from the reaction of naphthyl and acetylene at combustion-like temperatures. *Angew. Chem. Int. Edit.* **54,** 5421-5424 (2015).

22   Yang, T. *et al.* Hydrogen‐Abstraction/Acetylene‐Addition exposed. *Angew. Chem. Int. Edit.* **55,** 14983-14987 (2016).

23   Lorenz, R. D. & Lunine, J. I. Titan's surface reviewed: the nature of bright and dark terrain. *Planet. Space Sci.* **45,** 981-992 (1997).

24   Mebel, A. M., Landera, A. & Kaiser, R. I. Formation mechanisms of naphthalene and indene: From the interstellar medium to combustion flames. *J. Phys. Chem. A* **121,** 901-926 (2017).

25   Mebel, A. M., Georgievskii, Y., Jasper, A. W. & Klippenstein, S. J. Temperature-and pressure-dependent rate coefficients for the HACA pathways from benzene to naphthalene. *Proc. Combust. Inst.* **36,** 919-926 (2017).

26   Appel, J., Bockhorn, H. & Frenklach, M. Kinetic modeling of soot formation with detailed chemistry and physics: Laminar premixed flames of C_2 hydrocarbons. *Combust. Flame* **121,** 122-136 (2000).

27   Slavinskaya, N. A. & Frank, P. A modelling study of aromatic soot precursors formation in laminar methane and ethene flames. *Combust. Flame* **156,** 1705-1722 (2009).

28   Shukla, B. & Koshi, M. Comparative study on the growth mechanisms of PAHs. *Combust. Flame* **158,** 369-375 (2011).

29   Aguilera-Iparraguirre, J. & Klopper, W. Density functional theory study of the formation of naphthalene and phenanthrene from reactions of phenyl with vinyl-and phenylacetylene. *J. Chem. Theory Comput.* **3,** 139-145 (2007).

30   Yoon, Y. H. *et al.* The role of benzene photolysis in Titan haze formation. *Icarus* **233,** 233-241 (2014).

31   Vuitton, V., Yelle, R. V. & Lavvas, P. Composition and chemistry of Titan's thermosphere and ionosphere. *Philos. Trans. R. Soc., A* **367,** 729-741 (2009).

32   Gautier, T. *et al.* Nitrile gas chemistry in Titan's atmosphere. *Icarus* **213,** 625-635 (2011).

33   Imanaka, H. & Smith, M. A. Formation of nitrogenated organic aerosols in the Titan upper atmosphere. *Proc Natl Acad Sci U S A* **107,** 12423-12428 (2010).

34   Jacovi, R., Laufer, D., Dimitrov, V. & Bar-Nun, A. Chemical composition of simulated Titan's midatmospheric aerosols. *J. Geophys. Res.: Planets* **115,** E07006 (2010).

35   Kovács, T., Blitz, M. A. & Seakins, P. W. H-atom yields from the photolysis of acetylene and from the reaction of C_2H with H_2, C_2H_2, and C_2H_4. *J. Phys. Chem. A* **114,** 4735-4741 (2010).

36   Zhang, F., Kim, Y. S., Kaiser, R. I., Krishtal, S. P. & Mebel, A. M. Crossed molecular beams study on the formation of vinylacetylene in Titan's atmosphere. *J. Phys. Chem. A* **113,** 11167-11173 (2009).

37   Dimitrov, V. & Bar-Nun, A. Properties of the main high molecular weight hydrocarbons in Titan's atmosphere. *Prog. React. Kinet.* **22,** 67-81 (1997).

38   Dimitrov, V. & Bar-Nun, A. Kinetic pathways in the atmospheric chemistry of Titan - A generalized analysis. *Prog. React. Kinet. Mech.* **29,** 1-41 (2004).

39   Krasnopolsky, V. A. The photochemical model of Titan's atmosphere and ionosphere: A version without hydrodynamic escape. *Planet. Space Sci.* **58,** 1507-1515 (2010).

40   Yang, T. *et al.* HACA's heritage: A free-radical pathway to phenanthrene in circumstellar envelopes of asymptotic giant branch stars. *Angew. Chem. Int. Edit.* **56,** 4515-4519 (2017).

41   Hager, J. W. & Wallace, S. C. Two-laser photoionization supersonic jet mass spectrometry of aromatic molecules. *Anal. Chem.* **60,** 5-10 (1988).

42   Thantu, N. & Weber, P. M. Dependence of two-photon ionization photoelectron spectra on laser coherence bandwidth. *Chem. Phys. Lett.* **214,** 276-280 (1993).

43   Sebree, J. A. *et al.* Photochemistry of benzylallene: ring-closing reactions to form naphthalene. *J. Am. Chem. Soc.* **134,** 1153-1163 (2012).

44   Mebel, A. M., Lin, M. C., Yu, T. & Morokuma, K. Theoretical study of potential energy surface and thermal rate constants for the $C_6H_5+H_2$ and C_6H_6+H reactions. *J. Phys. Chem. A* **101,** 3189-3196 (1997).

45   Ali, A., Sittler, E. C., Chornay, D., Rowe, B. R. & Puzzarini, C. Organic chemistry in Titan′s upper atmosphere and its astrobiological consequences: I. Views towards Cassini plasma spectrometer (CAPS) and ion neutral mass spectrometer (INMS) experiments in space. *Planet. Space Sci.* **109-110,** 46-63 (2015).

46   Lindstedt, P., Maurice, L. & Meyer, M. Thermodynamic and kinetic issues in the formation and oxidation of aromatic species. *Faraday Discuss.* **119,** 409-432 (2002).

47   Zhang, F. *et al.* A VUV photoionization study of the formation of the indene molecule and its isomers. *J. Phys. Chem. Lett.* **2,** 1731-1735 (2011).

48   Zhang, F., Kaiser, R. I., Golan, A., Ahmed, M. & Hansen, N. A VUV photoionization study of the combustion-relevant reaction of the phenyl radical (C_6H_5) with propylene (C_3H_6) in a high temperature chemical reactor. *J. Phys. Chem. A* **116,** 3541-3546 (2012).

49   Parker, D. S. N., Kaiser, R. I., Kostko, O. & Ahmed, M. Selective formation of indene through the reaction of benzyl radicals with acetylene. *ChemPhysChem* **16,** 2091-2093 (2015).

50   Qi, F. Combustion chemistry probed by synchrotron VUV photoionization mass spectrometry. *Proc. Combust. Inst.* **34,** 33-63 (2013).

51   Cool, T. A. *et al.* Photoionization mass spectrometer for studies of flame chemistry with a synchrotron light source. *Rev. Sci. Instrum.* **76,** 094102 (2005).

52   Guan, Q. *et al.* The properties of a micro-reactor for the study of the unimolecular decomposition of large molecules. *Int. Rev. Phys. Chem.* **33,** 447-487 (2014).

53   Curtiss, L. A., Raghavachari, K., Redfern, P. C., Rassolov, V. & Pople, J. A. Gaussian-3 (G3) theory for molecules containing first and second-row atoms. *J. Chem. Phys.* **109,** 7764-7776 (1998).

54   Baboul, A. G., Curtiss, L. A., Redfern, P. C. & Raghavachari, K. Gaussian-3 theory using density functional geometries and zero-point energies. *J. Chem. Phys.* **110,** 7650-7657 (1999).

55   Curtiss, L. A., Raghavachari, K., Redfern, P. C., Baboul, A. G. & Pople, J. A. Gaussian-3 theory using coupled cluster energies. *Chem. Phys. Lett.* **314,** 101-107 (1999).

56   Frisch, M. J. *et al. Gaussian 09, revision A.02* **(Gaussian Inc., CT)** (2009).

57   Werner, H. J. *et al. MOLPRO, version 2010.1,* *http://www.molpro.net* **(University College Cardiff Consultants Ltd, United Kingdom)** (2010).

58   Georgievskii, Y., Miller, J. A., Burke, M. P. & Klippenstein, S. J. Reformulation and solution of the master equation for multiple-well chemical reactions. *J. Phys. Chem. A* **117,** 12146-12154 (2013).

Acknowledgments

Author contributions

R.I.K. designed the experiment; L.Z., B.X., and U.A. carried out the experimental measurements; M.A. supervised the experiment; L.Z. performed the data analysis; M.M.E., E.K.B., V.N.A. and A.M.M. carried out the theoretical analysis; R.I.K., A.M.M., and M.A. discussed the data; R.I.K. wrote the manuscript.

Competing financial interests

The authors declare no competing financial interests.

Data availability.

The data that support the plots within this paper and other findings of this study are available from the corresponding author upon reasonable request.
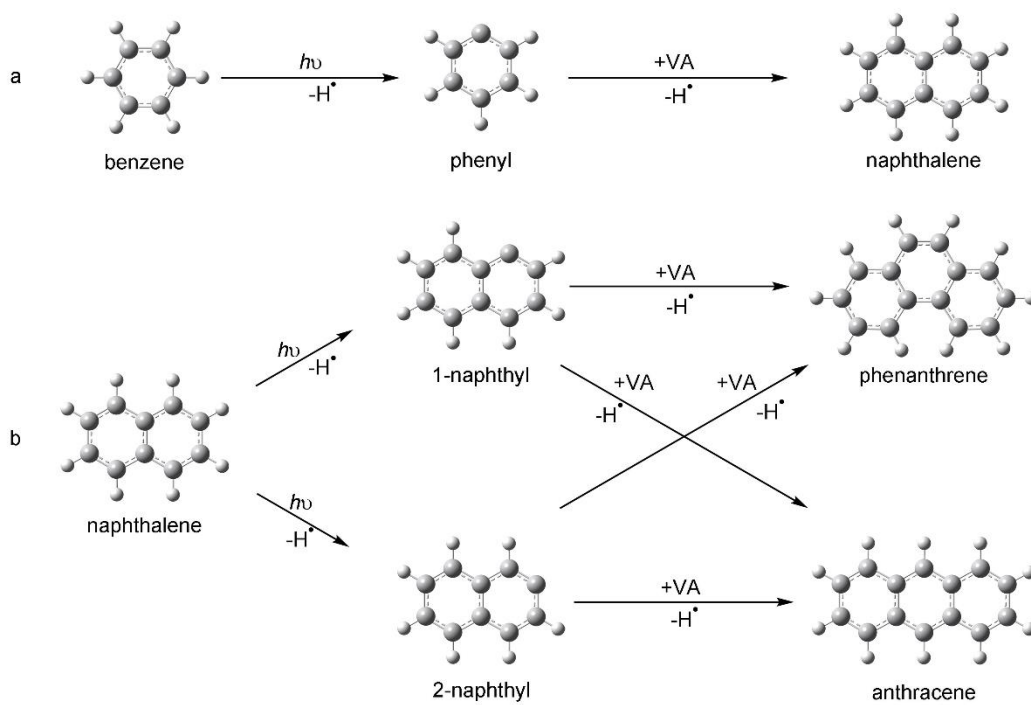
Figure 1. Schematic pathways involved in the synthesis of anthracene and phenanthrene. (a) Naphthalene formation via the reaction of phenyl radical ($C_6H_5^\bullet$) with vinylacetylene (C_4H_4, VA); (b) anthracene and phenanthrene formation via the reactions of 1- and 2-naphthyl radicals ($C_{10}H_7^\bullet$) with vinylacetylene.
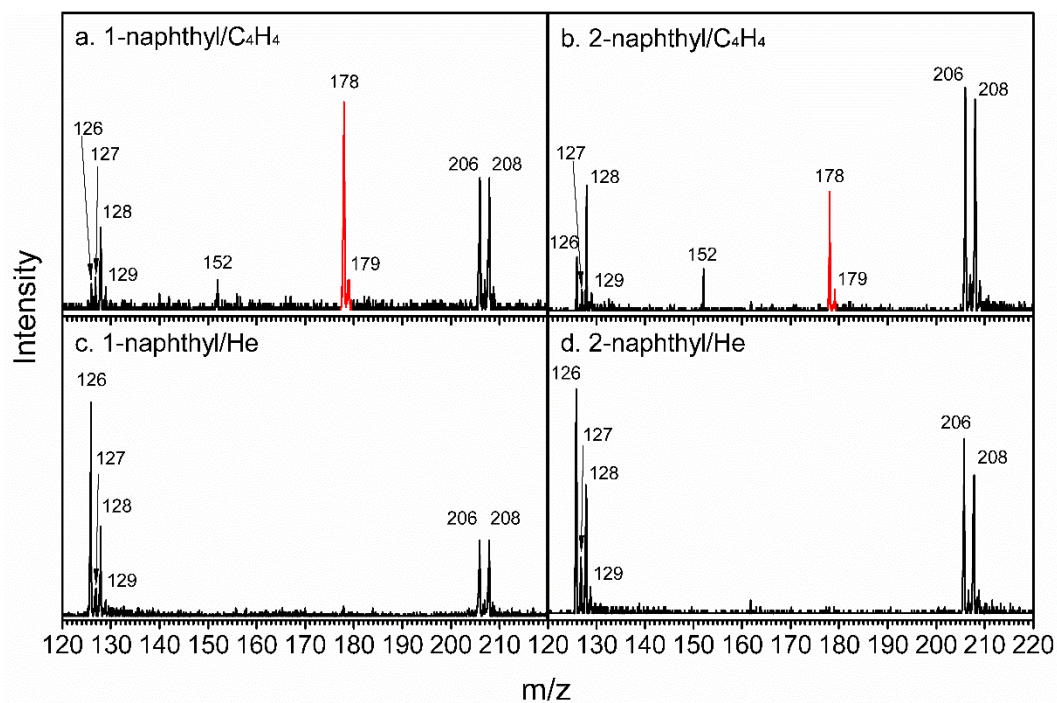
Figure 2. Comparison of the mass spectra recorded at a photoionization energy of 9.50 eV. (a) 1-naphthyl - vinylacetylene; (b) 2-naphthyl - vinylacetylene; (c) 1-naphthyl – helium, and (d) 2-naphthyl - helium systems. The peaks of the $C_{14}H_{10}$ isomer(s) ($m/z = 178$) along with the ^{13}C substituted counterparts ($m/z = 179$) are highlighted in red.
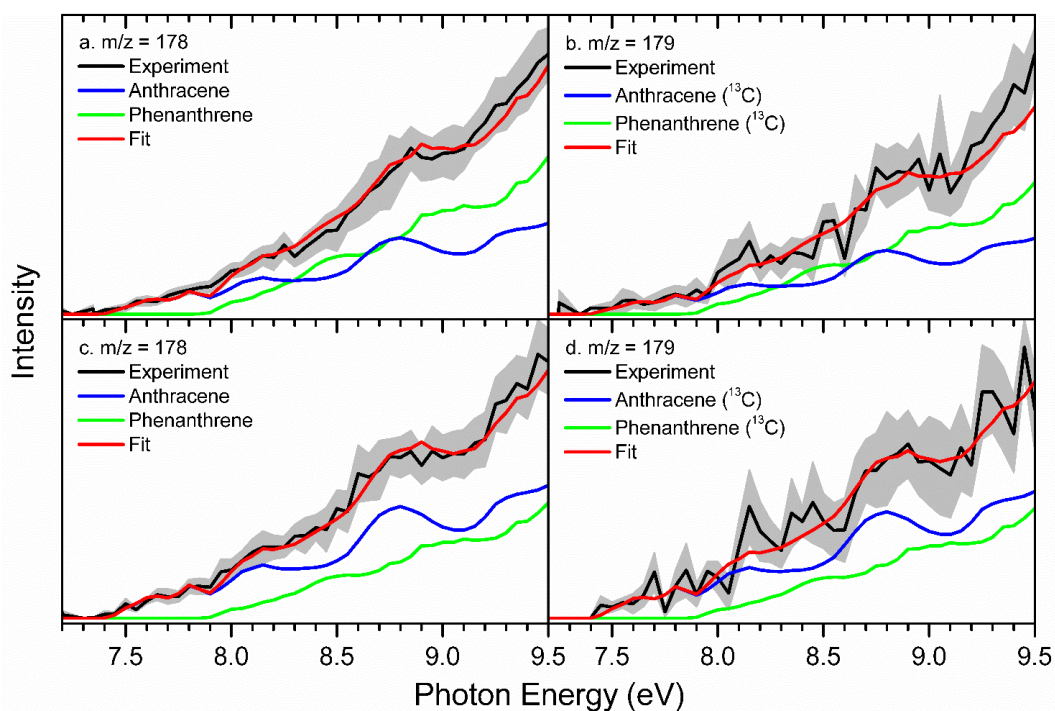
Figure 3. Photoionization efficiency (PIE) curves for ion counts recorded at *m/z* = 178 and 179. (a) and (b): 1-naphthyl - vinylacetylene system; (c) and (d): 2-naphthyl - vinylacetylene system. Black lines: experimentally derived PIE curves along with 1 σ error limits (gray area); blue lines: anthracene reference PIE; green lines: phenanthrene reference PIE; red lines: overall fit.
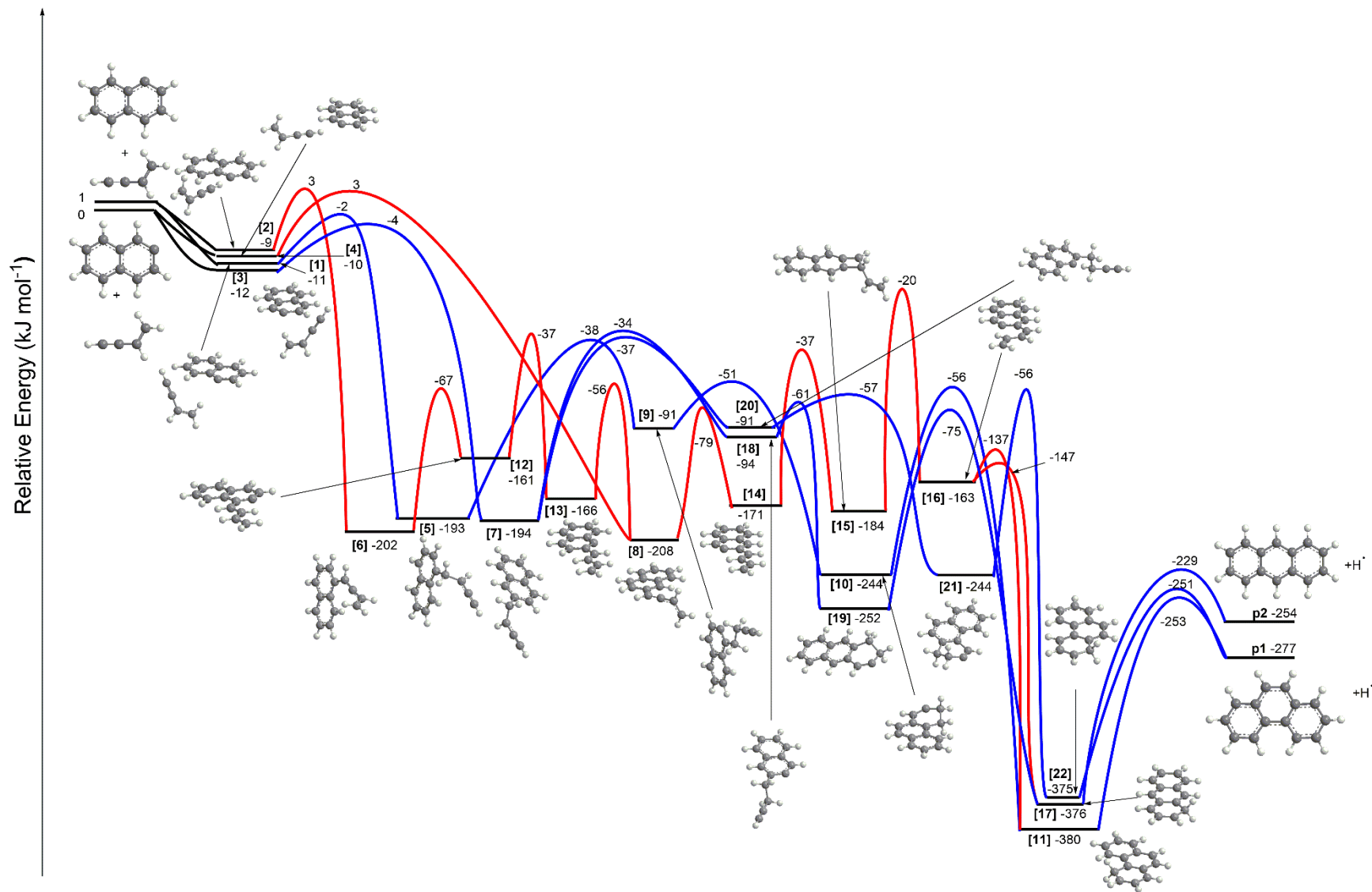
Figure 4. Potential energy surfaces of the reactions of 1-naphthyl and 2-naphthyl radicals with vinylacetylene leading to phenanthrene (p1) and anthracene (p2). The barrier-less reaction pathways highlighted in blue dominate the anthracene and phenanthrene formation in cold

environments such as in Titan's atmosphere. The pathways denoted in red have entrance barriers and hence are only relevant at elevated temperatures as present, for instance, in combustion flames, but closed at low temperatures due to the inherent barriers to reaction. Optimized Cartesian coordinates for all structures and a full version of this surface including the pathways to substituted naphthalene isomers and hydrogen abstraction yielding naphthalene are compiled in the Supplementary Information. Also, the initial covalently bound intermediates [5]-[8] can immediately lose a hydrogen atom from the attacking C1 or C4 atoms of vinylacetylene to form naphthylvinylacetylene isomers 1-naphthyl-vinylacetylene-4 (1-((E)-but-1-en-3-ynyl)naphthalene, $C_{10}H_7HCCHCCH$; p4), 1-naphthyl-vinylacetylene-1 (1-(but-3-en-1-ynyl)naphthalene, $C_{10}H_7CCC_2H_3$; p3), 2-naphthyl-vinylacetylene-4 (2-((E)-but-1-en-3-ynyl) naphthalene, $C_{10}H_7HCCHCCH$; p6), and 2-naphthyl-vinylacetylene-1 (2-(but-3-en-1-ynyl)naphthalene, $C_{10}H_7CCC_2H_3$; p5), respectively. These products are thermodynamically less stable than anthracene and phenanthrene, and their formation is not competitive at low temperatures characteristic to Titan, but they may prevail in combustion environments as the primary reaction products due to entropic favorability of the hydrogen atom loss.

Low-Temperature Formation of Polycyclic Aromatic Hydrocarbons in Titan's Atmosphere

Long Zhao, Ralf I. Kaiser*

Department of Chemistry, University of Hawaii at Manoa, Honolulu, Hawaii, 96822

Bo Xu, Utuq Ablikim, Musahid Ahmed*

Chemical Sciences Division, Lawrence Berkeley National Laboratory, Berkeley, California 94720,
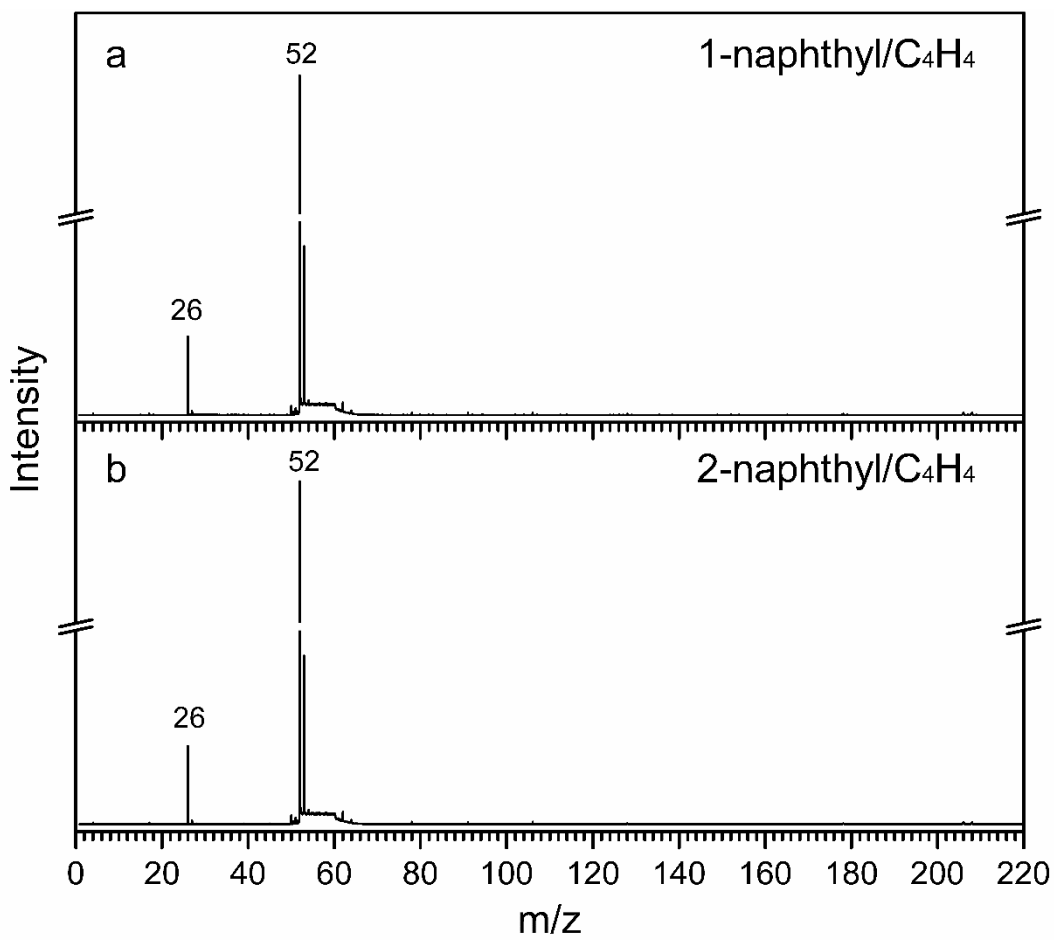

Mikhail M. Evseev, Eugene K. Bashkirov, Valeriy N. Azyazov

Samara University, Samara, 443086, Russia

Alexander M. Mebel*

Department of Chemistry and Biochemistry, Florida International University, Miami, Florida 33199

and Samara University, Samara, 443086, Russia

Supplementary Figure 1. Photoionization mass spectra recorded at a photoionization energy of 12.0 eV for the (a) 1-naphthyl ($C_{10}H_7^\bullet$) - vinylacetylene (C_4H_4) and (b) 2-naphthyl ($C_{10}H_7^\bullet$) - vinylacetylene (C_4H_4) systems. Note that at high temperatures, vinylacetylene can decompose to acetylene at fractions of about 2%[1,2]. The photoionization energy of acetylene is 11.4 eV[3]. Mass spectra at photoionization energies of 12.0 eV were recorded to identify acetylene. Acetylene can react with naphthyl radicals to yield acenaphthylene ($C_{12}H_8$) (m/z = 152) as demostrated by Parker et al.[4]
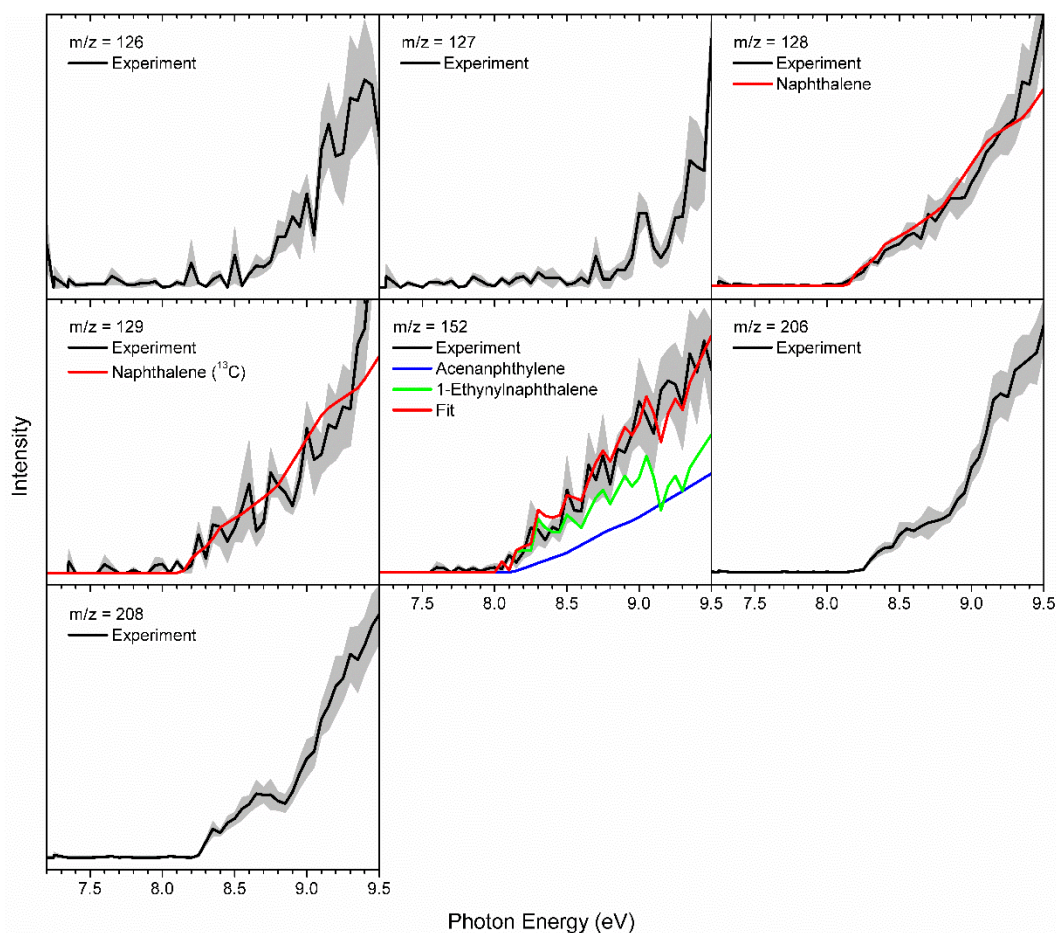
Supplementary Figure 2. Supplementary photoionization efficiency curves (PIEs, black lines) recorded in the 1-naphthyl - vinylacetylene reaction. The black lines represent the experimental data along with the experimental errors denoted in gray areas; the reference PIE curves are color coded in blue, green, and red lines. In case of multiple contributions to one PIE curve, the red line resembles the overall fit. The species at $m/z = 127$ is identified as the 1-naphthyl radical ($C_{10}H_7^{\bullet}$) generated from the pyrolysis of the precursor 1-bromonaphthalene. Ions at $m/z = 126$ and 128 are associated to the atomic hydrogen loss and addition to and from the 1-naphthyl radical, respectively. Signal at $m/z = 128$ is identified as naphthalene, and $m/z = 129$ as ^{13}C-naphthalene. The ions at $m/z = 152$ are attributed to acenaphthylene ($C_{12}H_8$) and ethynylnaphthalene isomers ($C_{12}H_8$). Signals at $m/z = 206$ and 208 are attributed to the precursor 1-bromonaphthalene ($C_{10}H_7{}^{79}Br$ and $C_{10}H_7{}^{81}Br$).
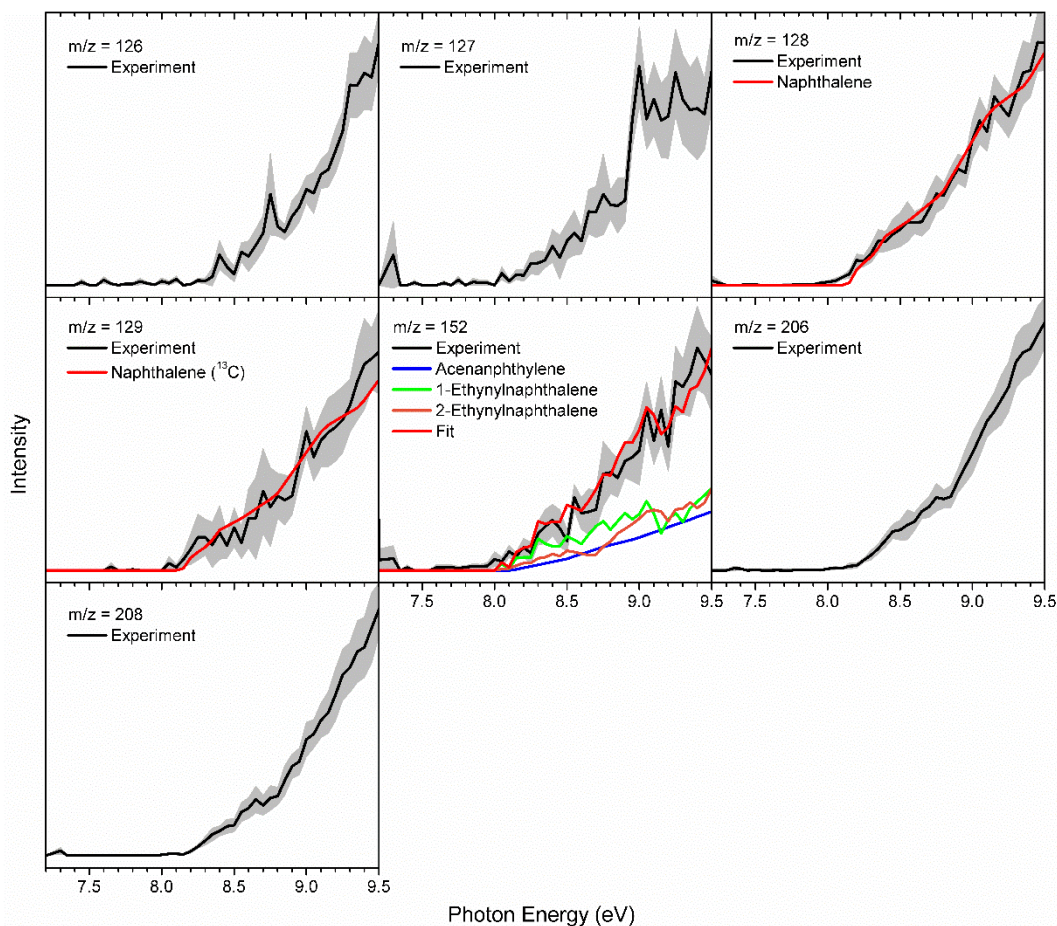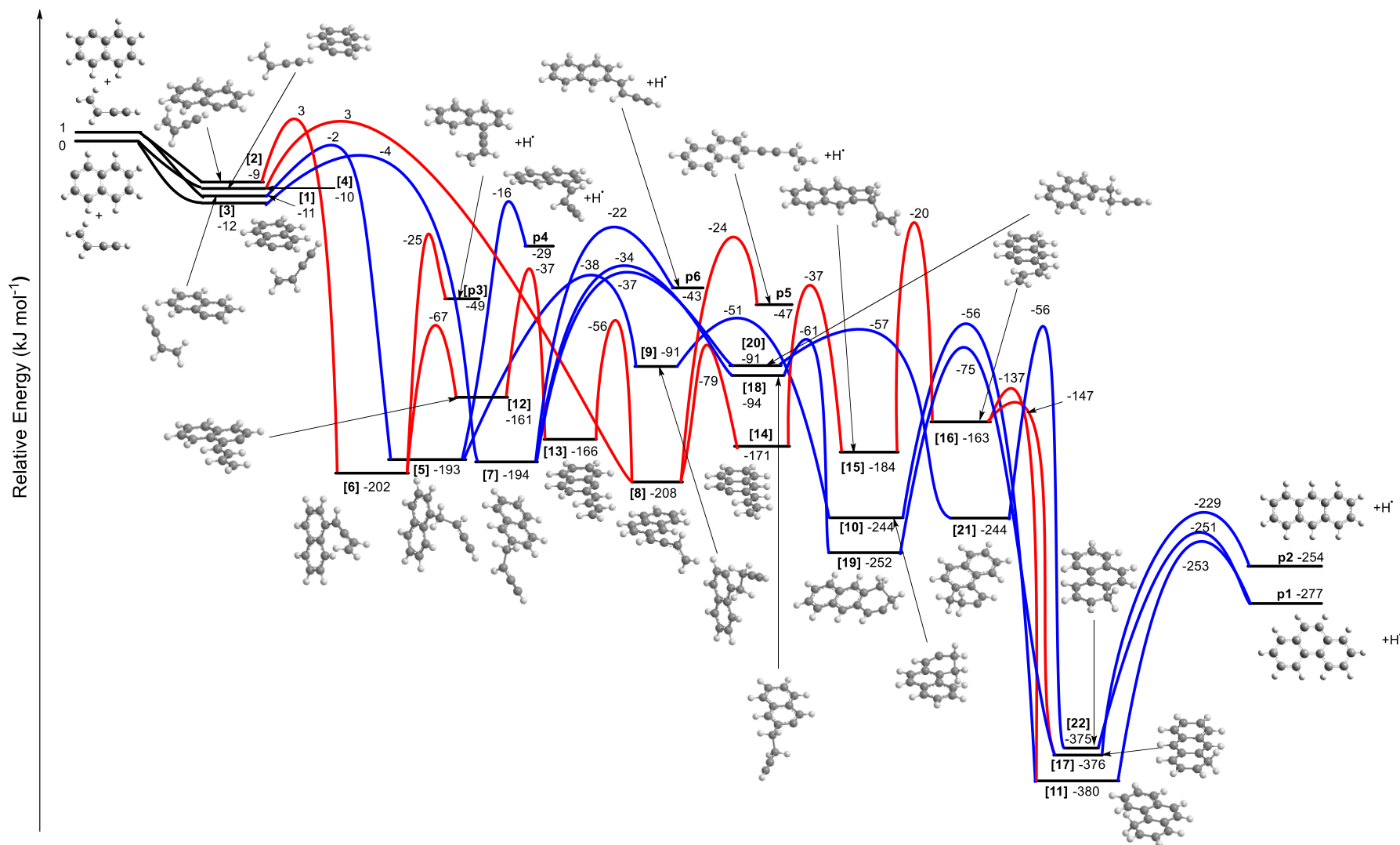
Supplementary Figure 3. Supplementary photoionization efficiency curves (PIEs, black lines) recorded in the 2-naphthyl - vinylacetylene reaction. The black lines represent the experimental data along with the experimental errors denoted in gray areas; the reference PIE curves are color coded in blue, green, and red lines. In case of multiple contributions to one PIE curve, the red line resembles the overall fit. The species at m/z = 127 is identified as the 2-naphthyl radical ($C_{10}H_7^\bullet$) generated from the pyrolysis of the precursor 2-bromonaphthalene. Ions at m/z = 126 and 128 are associated to the atomic hydrogen loss and addition to and from the 2-naphthyl radical, respectively. Signal at m/z = 128 is identified as naphthalene, and m/z = 129 as ^{13}C-naphthalene. The ions at m/z = 152 are attributed to acenaphthylene ($C_{12}H_8$) and ethynylnaphthalene isomers ($C_{12}H_8$). Signals at m/z = 206 and 208 are attributed to the precursor 1-bromonaphthalene ($C_{10}H_7^{79}Br$ and $C_{10}H_7^{81}Br$).
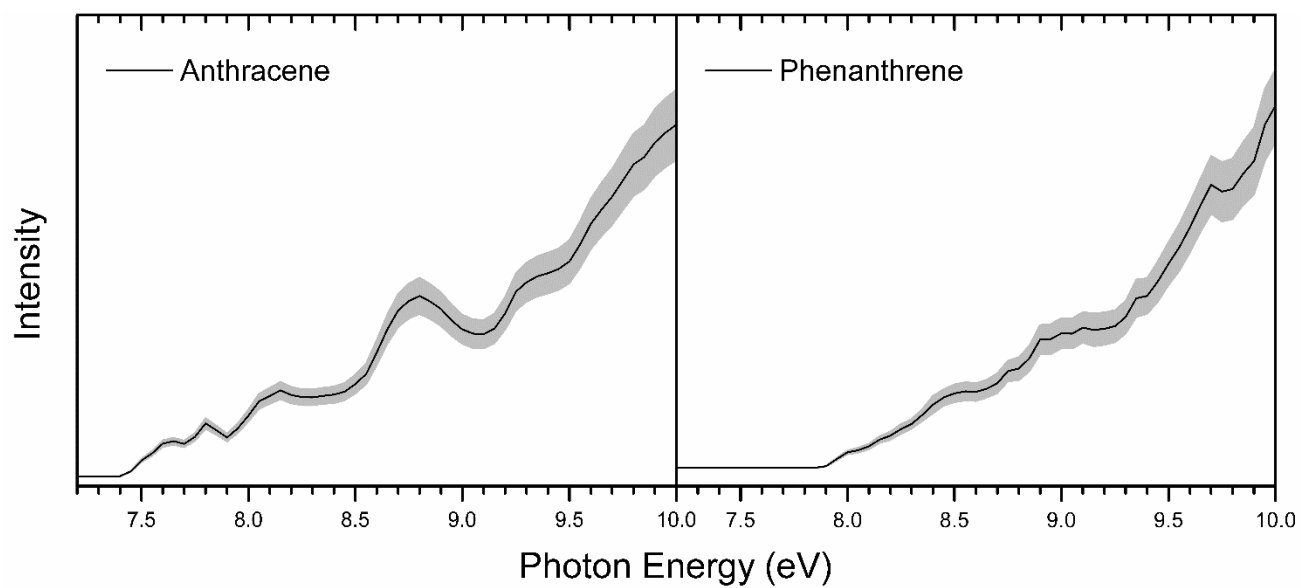
Supplementary Figure 4. PIE calibration curves for anthracene and phenanthrene collected in this work. The ionization energies of anthracene and phenanthrene are 7.40 ± 0.05 eV and 7.85 ± 0.05 eV, respectively, corresponding well with the reported adiabatic photoionization energies of 7.44[5] and 7.90 eV[6].

Supplementary Figure 5. Complete potential energy surfaces of the reactions of 1-naphthyl and 2-naphthyl radicals with vinylacetylene. Besides the 14-π-electron aromatic molecules anthracene (**p1**) and phenanthrene (**p2**) discussed in the manuscript, the doublet intermediates [5] – [8]

formed upon initial addition of the naphthyl radicals to vinylacetylene can also undergo unimolecular decomposition via hydrogen atom loss yielding four thermodynamically less stable naphthyl-vinylacetylene isomers: 1-naphthyl-vinylacetylene-1 ($C_{10}H_7CCC_2H_3$; **p3**), 1-naphthyl-vinylacetylene-4 ($C_{10}H_7HCCHCCH$; **p4**), 2-naphthyl-vinylacetylene-1 ($C_{10}H_7CCC_2H_3$; **p5**), and 2-naphthyl-vinylacetylene-4 ($C_{10}H_7HCCHCCH$; **p6**) in overall weakly exoergic reactions from 29 to 49 kJ mol^{-1}.

Supplementary Table 1. Rate constants (cm^3 s^{-1}) and branching fractions of various products in the reactions of 1- and 2-naphthyl radicals with C$_4$H$_4$ under Titan's atmospheric conditions (10^{-8} bar at 800 km altitude).

	1-naphthyl + C$_4$H$_4$ → phenanthrene + H _p_, bar					
_T_, K	1.00E-15	1.00E-10	1.00E-08	1.00E-06	0.0001	0.01
70	1.46E-15	1.14E-15	7.86E-18	1.20E-21	1.21E-25	5.10E-30
80	9.29E-16	7.36E-16	5.72E-18	8.93E-22	9.01E-26	4.18E-30
90	7.09E-16	5.72E-16	5.02E-18	8.02E-22	8.13E-26	4.13E-30
100	6.18E-16	5.07E-16	5.06E-18	8.25E-22	8.40E-26	4.64E-30
110	5.94E-16	4.94E-16	5.64E-18	9.42E-22	9.64E-26	5.76E-30
120	6.14E-16	5.18E-16	6.82E-18	1.17E-21	1.20E-25	7.73E-30
130	6.73E-16	5.76E-16	8.81E-18	1.54E-21	1.61E-25	1.10E-29
140	7.71E-16	6.68E-16	1.20E-17	2.16E-21	2.28E-25	1.66E-29
150	9.14E-16	8.03E-16	1.71E-17	3.17E-21	3.39E-25	2.61E-29
160	1.11E-15	9.88E-16	2.51E-17	4.84E-21	5.28E-25	4.25E-29
170	1.38E-15	1.24E-15	3.79E-17	7.66E-21	8.54E-25	7.16E-29
180	1.73E-15	1.57E-15	5.83E-17	1.25E-20	1.43E-24	1.24E-28
_T_, K	0.03	0.1	0.3	1	3	
70	1.49E-31	1.76E-33	2.44E-35	2.06E-37	2.58E-39	
80	1.31E-31	1.62E-33	2.29E-35	1.94E-37	2.43E-39	
90	1.40E-31	1.82E-33	2.62E-35	2.24E-37	2.81E-39	
100	1.70E-31	2.35E-33	3.47E-35	3.00E-37	3.78E-39	
110	2.30E-31	3.41E-33	5.18E-35	4.53E-37	5.73E-39	
120	3.37E-31	5.39E-33	8.49E-35	7.55E-37	9.59E-39	
130	5.25E-31	9.14E-33	1.51E-34	1.37E-36	1.74E-38	
140	8.61E-31	1.65E-32	2.85E-34	2.65E-36	3.41E-38	
150	1.47E-30	3.11E-32	5.70E-34	5.46E-36	7.11E-38	
160	2.61E-30	6.08E-32	1.19E-33	1.19E-35	1.56E-37	
170	4.74E-30	1.23E-31	2.59E-33	2.69E-35	3.59E-37	
180	8.81E-30	2.53E-31	5.77E-33	6.29E-35	8.59E-37	

	2-naphthyl + C$_4$H$_4$ $\rightarrow$ anthracene/phenanthrene + H $\quad$ p, bar											
	1.00E-15		**1.00E-10**		**1.00E-08**		**1.00E-06**		**0.0001**		**0.01**	
T, K	Anthr.	Phenan.	Anthr.	Phenan.	Anthr.	Phenan.	Anthr.	Phenan.	Anthr.	Phenan.	Anthr.	Phenan.
70	7.38E-15	8.49E-16	6.24E-15	6.59E-16	1.13E-16	4.31E-18	1.85E-20	6.07E-22	1.86E-24	6.09E-26	1.15E-29	2.66E-30
80	4.19E-15	5.19E-16	3.59E-15	4.10E-16	7.50E-17	3.02E-18	1.28E-20	4.33E-22	1.29E-24	4.36E-26	8.93E-30	2.07E-30
90	2.88E-15	3.88E-16	2.49E-15	3.12E-16	6.05E-17	2.60E-18	1.08E-20	3.78E-22	1.09E-24	3.82E-26	8.53E-30	1.97E-30
100	2.27E-15	3.35E-16	1.99E-15	2.73E-16	5.59E-17	2.58E-18	1.05E-20	3.82E-22	1.07E-24	3.88E-26	9.42E-30	2.16E-30
110	1.98E-15	3.21E-16	1.74E-15	2.66E-16	5.71E-17	2.87E-18	1.14E-20	4.32E-22	1.16E-24	4.41E-26	1.16E-29	2.64E-30
120	1.85E-15	3.36E-16	1.65E-15	2.82E-16	6.29E-17	3.48E-18	1.34E-20	5.33E-22	1.38E-24	5.47E-26	1.57E-29	3.51E-30
130	1.84E-15	3.73E-16	1.65E-15	3.18E-16	7.33E-17	4.53E-18	1.70E-20	7.06E-22	1.77E-24	7.31E-26	2.27E-29	4.99E-30
140	1.92E-15	4.38E-16	1.73E-15	3.78E-16	8.92E-17	6.25E-18	2.27E-20	9.93E-22	2.39E-24	1.04E-25	3.50E-29	7.50E-30
150	2.07E-15	5.33E-16	1.88E-15	4.66E-16	1.12E-16	9.05E-18	3.19E-20	1.47E-21	3.41E-24	1.56E-25	5.69E-29	1.18E-29
160	2.30E-15	6.70E-16	2.11E-15	5.92E-16	1.45E-16	1.36E-17	4.68E-20	2.28E-21	5.07E-24	2.45E-25	9.65E-29	1.94E-29
170	2.60E-15	8.57E-16	2.41E-15	7.66E-16	1.91E-16	2.11E-17	7.09E-20	3.66E-21	7.85E-24	4.00E-25	1.70E-28	3.30E-29
180	3.02E-15	1.12E-15	2.81E-15	1.01E-15	2.54E-16	3.33E-17	1.11E-19	6.08E-21	1.26E-23	6.76E-25	3.10E-28	5.77E-29
	0.03		**0.1**		**0.3**		**1**		**3**			
T, K	Anthr.	Phenan.	Anthr.	Phenan.	Anthr.	Phenan.	Anthr.	Phenan.	Anthr.	Phenan.		
70	2.54E-31	8.17E-32	2.76E-33	9.87E-34	3.75E-35	1.38E-35	3.15E-37	1.17E-37	3.93E-39	1.46E-39		
80	2.06E-31	6.81E-32	2.31E-33	8.59E-34	3.19E-35	1.22E-35	2.70E-37	1.04E-37	3.37E-39	1.30E-39		
90	2.05E-31	6.97E-32	2.39E-33	9.22E-34	3.36E-35	1.33E-35	2.85E-37	1.14E-37	3.57E-39	1.43E-39		
100	2.37E-31	8.25E-32	2.88E-33	1.15E-33	4.11E-35	1.70E-35	3.52E-37	1.47E-37	4.42E-39	1.85E-39		
110	3.06E-31	1.09E-31	3.89E-33	1.63E-33	5.68E-35	2.46E-35	4.91E-37	2.15E-37	6.18E-39	2.72E-39		
120	4.33E-31	1.58E-31	5.76E-33	2.52E-33	8.65E-35	3.94E-35	7.57E-37	3.48E-37	9.56E-39	4.41E-39		
130	6.57E-31	2.44E-31	9.22E-33	4.23E-33	1.43E-34	6.84E-35	1.27E-36	6.14E-37	1.61E-38	7.82E-39		
140	1.06E-30	4.00E-31	1.57E-32	7.55E-33	2.52E-34	1.27E-34	2.28E-36	1.17E-36	2.91E-38	1.49E-38		
150	1.80E-30	6.85E-31	2.83E-32	1.42E-32	4.72E-34	2.52E-34	4.35E-36	2.36E-36	5.60E-38	3.04E-38		
160	3.20E-30	1.22E-30	5.34E-32	2.79E-32	9.29E-34	5.24E-34	8.78E-36	5.03E-36	1.14E-37	6.55E-38		
170	5.90E-30	2.23E-30	1.05E-31	5.66E-32	1.91E-33	1.13E-33	1.85E-35	1.13E-35	2.43E-37	1.48E-37		
180	1.12E-29	4.18E-30	2.11E-31	1.18E-31	4.05E-33	2.53E-33	4.07E-35	2.61E-35	5.40E-37	3.48E-37		

S9

Modeling Complications: To explore the effects of a stepwise, vinylacetylene-mediated formation of PAHs in Titan's atmosphere quantitatively, atmospheric modeling would be beneficial. Even a simplified one-dimensional model would require three sets of input parameters. These are i) the aryl radical reactants (phenyl ($C_6H_5^•$), naphthyl ($C_{10}H_7^•$), anthracenyl ($C_{14}H_9^•$), phenanthrenyl ($C_{14}H_9^•$)) formed via photodissociation of benzene (C_6H_6), naphthalene ($C_{10}H_8$), anthracene ($C_{14}H_{10}$), and phenanthrene ($C_{14}H_{10}$) from the solar radiation field, ii) the reaction products, and iii) temperature and pressure dependent rate constants along with their branching ratios. A literature research failed to provide any experimental low temperature rate, pressure–dependent constants for the reactions of vinylacetylene with the aryl radicals. The calculated temperature-and pressure-dependent rate constants over Titan's relevant temperature range of 70 K to 180 K covering pressures from 10^{-15} to 3 bar are presented in Supplementary Information. Their values indicate that indeed, the formation of phenanthrene and anthracene from 1- and 2-naphthyl radical should be feasible at very low pressures up to 10^{-8} bar. However, considering the sensitivity of the rate constants to the heights of the submerged barrier and the resulting range of rate constants covering two orders of magnitude for 1-/2-naphthyl plus vinylacetylene and even for the simplest phenyl – vinylacetylene system[7], experimental validation of the calculated rate constants is highly desirable. Likewise, wavelength-dependent, absolute photodissociation cross sections of naphthalene, anthracene, and phenanthrene leading to the corresponding aryl radicals are not available and need to be measured or accurately evaluated theoretically. Finally, while the reaction products of the phenyl and 1-/2-naphthyl radical reactions with vinylacetylene are known[8], those of the phenanthrenyl-vinylacetylene and anthra-cenyl-vinylacetylene systems are lacking. Based on the aforementioned reaction mechanisms, anthracene and phenanthrene have three and five chemically non-equivalent hydrogen atoms respectively, which when photodissociated to three and five chemically distinct anthracenyl and phenanthrenyl radicals can subsequently serve as aryl reactants with vinylacetylene leading to five $C_{18}H_{12}$ isomers carrying four six-membered rings (benz[*a*]anthracene, tetracene, chrysene, benzo[*c*]phenanthrene and triphenylene) (Supplementary Figure 6). PAH formation might also involve ion-molecule reactions in the upper atmosphere[9]. Therefore, both neutral-neutral and ion-molecule reactions might produce PAHs, but the effectiveness of these processes depends on the temperature and pressure, with neutral-neutral reactions dominating in lower atmospheric layers where ions are absent, but photons can still penetrate to cleave carbon-hydrogen bonds of organic molecules forming the desired aryl radicals. This likely results in depth-dependent PAH production routes. Finally, Titan's hydrocarbon and nitrogen chemistries are strongly coupled; these processes might even lead to nitrogen substituted PAHs such as (iso)quinolone; their successive chemical

reaction and photochemical properties are only beginning to emerge[10-16], but a systematic understanding is unknown as of now, but critical to establish predictive photochemical models. Therefore, at this stage we did not attempt to develop an atmospheric model of PAH formation in Titan's atmosphere due to the lack of critical input parameters detailed above.

PAH-type Molecules for Titan's Atmosphere

Within this work, it is critical to highlight that the origin of heavy ions in the ionosphere and their implications for prebiotic chemistry,[17] the incorporation of nitrogen into a carbon network,[17,18] and the subsequent transition from the initial building blocks of PAH-type molecules toward aerosols and haze formation on Titan remains a much debated topic. Due to the lack of observational probes of Titan's atmosphere at the most fundamental, molecular level encompassing moderately large molecules and aerosols, the planetary science community turned to laboratory based measurements to simulate haze and aerosol formation on Titan.[19-21] A key component of these experiments has been the photodissociation of gas phase mixtures incorporating, for instance, methane (CH_4) and nitrogen (N_2) and subsequent analysis of the complex molecules that originate in these experiments most notably with infrared and mass spectrometry. While CH_4/N_2 mixtures resulted in high molecular weight polymers incorporating PAHs and polyphenyl type systems, seeding these mixtures with trace aromatic compounds like benzene and naphthalene gave rise to PAH-based ring structures reminiscent of a free radical chemistry such as via phenyl and naphthyl radicals prevalent in combustion environments.[20] Hence, our studies support that free radical based chain reactions could synthesize PAH systems, which act as nuclei for particle growth in Titan's atmosphere.
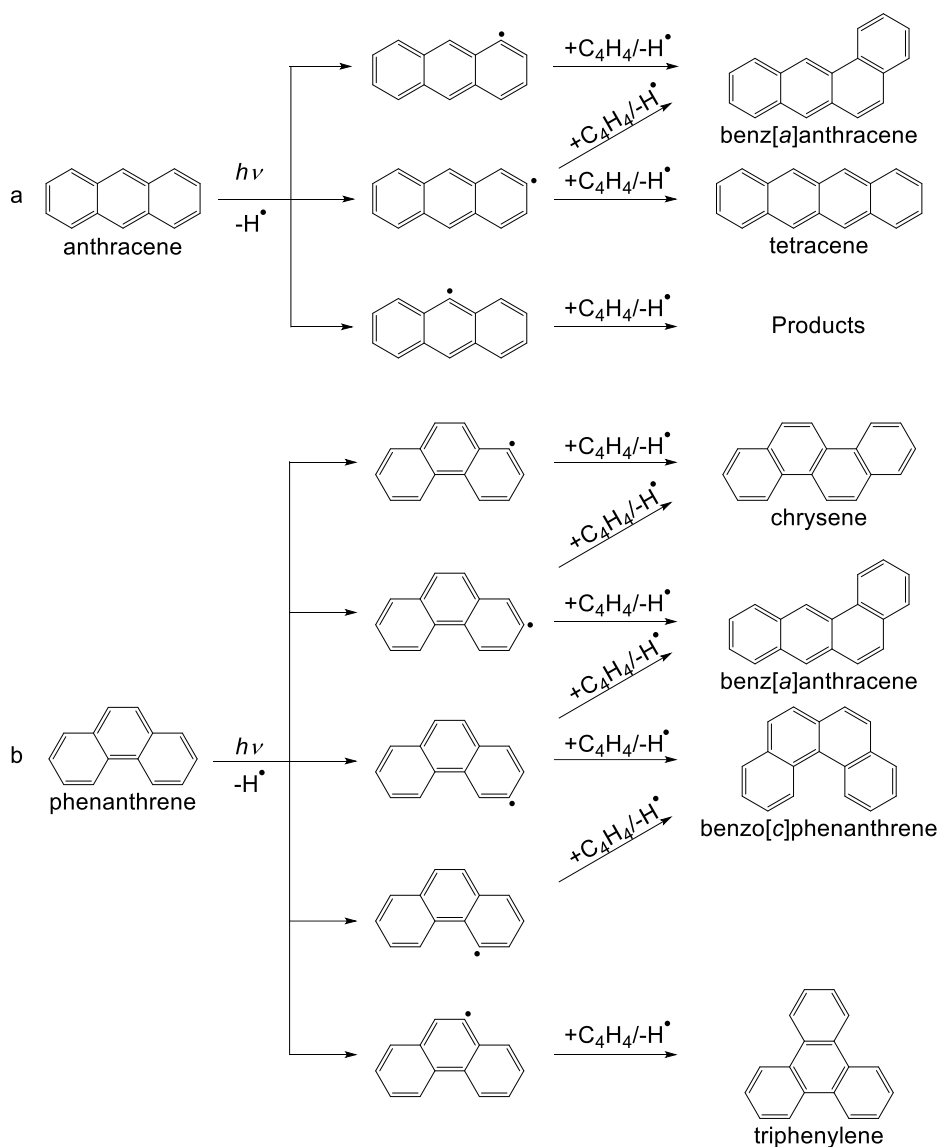
Supplementary Figure 6. Formation of PAH carrying four six-member rings initiated by anthracene (a) and phenanthrene (b) photodissociation accompanied by atomic hydrogen loss. Starting from anthracene and phenanthrene, three anthracenyl and five phenanthrenyl radicals can be produced via photodissociation. Reacting with vinylacetylene, these aryl radicals can yield five $C_{18}H_{12}$ isomers carrying four six-membered rings, which are benz[a]anthracene, tetracene, chrysene, benzo[c]phenanthrene and triphenylene.

References

1   Hidaka, Y., Tanaka, K. & Suga, M. Thermal decomposition of vinylacetylene in shock waves: Rate constant of initiation reaction. *Chem. Phys. Lett.* **130,** 195-198 (1986).

2   Colket, M. B. The Pyrolysis of Acetylene and Vinylacetylene in a Single-Pulse Shock Tube. *Proc. Combust. Inst.* **21,** 851-864 (1988).

3   Cool, T. A., Wang, J., Nakajima, K., Taatjes, C. A. & McIlroy, A. Photoionization cross sections for reaction intermediates in hydrocarbon combustion. *Int. J. Mass spectrom.* **247,** 18-27 (2005).

4   Parker, D. S. N. *et al.* Unexpected chemistry from the reaction of naphthyl and acetylene at combustion-like temperatures. *Angew. Chem. Int. Edit.* **54,** 5421-5424 (2015).

5   Hager, J. W. & Wallace, S. C. Two-laser photoionization supersonic jet mass spectrometry of aromatic molecules. *Anal. Chem.* **60,** 5-10 (1988).

6   Thantu, N. & Weber, P. M. Dependence of two-photon ionization photoelectron spectra on laser coherence bandwidth. *Chem. Phys. Lett.* **214,** 276-280 (1993).

7   Mebel, A. M., Landera, A. & Kaiser, R. I. Formation mechanisms of naphthalene and indene: From the interstellar medium to combustion flames. *J. Phys. Chem. A* **121,** 901-926 (2017).

8   Parker, D. S. *et al.* Low temperature formation of naphthalene and its role in the synthesis of PAHs (polycyclic aromatic hydrocarbons) in the interstellar medium. *Proc. Natl. Acad. Sci. USA* **109,** 53-58 (2012).

9   Ali, A., Sittler, E. C., Chornay, D., Rowe, B. R. & Puzzarini, C. Organic chemistry in Titan's upper atmosphere and its astrobiological consequences: I. Views towards Cassini plasma spectrometer (CAPS) and ion neutral mass spectrometer (INMS) experiments in space. *Planet. Space Sci.* **109-110,** 46-63 (2015).

10   Landera, A. & Mebel, A. M. Low-temperature mechanisms for the formation of substituted azanaphthalenes through consecutive CN and C_2H additions to styrene and N-methylenebenzenamine: a theoretical study. *J. Am. Chem. Soc.* **135,** 7251-7263 (2013).

11   Bouwman, J., Sztaray, B., Oomens, J., Hemberger, P. & Bodi, A. Dissociative photoionization of quinoline and isoquinoline. *J. Phys. Chem. A* **119,** 1127-1136 (2015).

12   Sciamma-O'Brien, E., Ricketts, C. L. & Salama, F. The Titan Haze Simulation experiment on COSmIC: Probing Titan's atmospheric chemistry at low temperature. *Icarus* **243,** 325-336 (2014).

13   Soliman, A.-R., Attah, I. K., Hamid, A. M. & El-Shall, M. S. Growth kinetics and formation mechanisms of complex organics by sequential reactions of acetylene with ionized aromatics. *Int. J. Mass Spectrom.* **377,** 139-151 (2015).

14   Westlake, J. H., Waite, J. H., Jr., Carrasco, N., Richard, M. & Cravens, T. The role of ion-molecule reactions in the growth of heavy ions in Titan's ionosphere. *J. Geophys. Res.: Space Phys.* **119,** 5951-5963 (2014).

15   Lopez-Puertas, M. *et al.* Large abundances of polycyclic aromatic hydrocarbons in Titan's upper atmosphere. *Astrophys. J.* **770,** 132-139 (2013).

16   Landera, A. & Mebel, A. M. Mechanisms of formation of nitrogen-containing polycyclic aromatic compounds in low-temperature environments of planetary atmospheres: a theoretical study. *Faraday Discuss.* **147,** 479-494 (2010).

17   Saladino, R. *et al.* First evidence on the role of heavy ion irradiation of meteorites and formamide in the origin of biomolecules. *Orig Life Evol Biosph* **46,** 515-521 (2016).

18   Imanaka, H. *et al.* Laboratory experiments of Titan tholin formed in cold plasma at various pressures: implications for nitrogen-containing polycyclic aromatic compounds in Titan haze. *Icarus* **168,** 344-366 (2004).

19   Horst, S. M. *et al.* Laboratory investigations of Titan haze formation: In situ measurement of gas and particle composition. *Icarus* **301,** 136-151 (2018).

20   Gautier, T. *et al.* Influence of trace aromatics on the chemical growth mechanisms of Titan aerosol analogues. *Planet. Space Sci.* **140,** 27-34 (2017).

21   Yoon, Y. H. *et al.* The role of benzene photolysis in Titan haze formation. *Icarus* **233,** 233-241 (2014).